Low Temperature Physics/Fizika Nizkikh Temperatur, 2020, v. 46, No. 3, pp. 322–327

Differential entropy per particle in Dirac semimetals in external magnetic field

I.V. Sukhenko, S.G. Sharapov, and V.P. Gusynin

Bogolyubov Institute for Theoretical Physics, National Academy of Science of Ukraine
14-b Metrolohichna Street, Kyiv 03143, Ukraine
E-mail: sharapov@bitp.kiev.ua

Received December 2, 2019, published online January 27, 2020

We obtain a general expression for the differential entropy per particle (DEP) for three-dimensional Dirac systems as a function of chemical potential, temperature and magnetic field. It is shown that in the presence of magnetic field the dependence of DEP on the chemical potential near a charge neutral point is quite different from the corresponding dependence in graphene. Specifically, we observe a flat region with almost zero DEP near the charge neutral point which grows with the increase of the magnetic field followed then by decreasing oscillations due to contributions from the Landau levels. In contrast, in graphene there is a sharp peak observed for the chemical potential in the temperature vicinity of the Dirac point.

Keywords: 3D Dirac systems, differential entropy, chemical potential, magnetic field.

1. Introduction

Entropy of many-body systems plays a fundamental role characterizing their thermodynamical, heat transfer and thermoelectric properties, however, it is always hard to measure it directly. The experiment presented in [1] is not an exception, because the directly measured quantity is temperature derivative of the chemical potential, $\partial\mu/\partial T$. This technique allowed to study two-dimensional (2D) electron gas with a three orders of magnitude higher resolution than the other methods, and thus it can be very helpful in probing interaction effects in 2D electron systems. The experiment [1] is based on the idea that modulation of the sample temperature changes the chemical potential and, hence, causes recharging of the gated structure, where the 2D electrons and the gate act as two plates of a capacitor. Thus, $\partial\mu/\partial T$ is directly extracted from the measured recharging current.

The differential entropy per particle (DEP), $s=\partial S/\partial n$, where S is the entropy per unit volume and n is the electron density, is then found from the Maxwell relation

$$s=\left(\frac{\partial S}{\partial n}\right)_T=-\left(\frac{\partial \mu}{\partial T}\right)_n. \qquad (1)$$

The quantized peaks of the entropy per electron in a quasi-two-dimensional electron gas with a parabolic dispersion were recently studied in [2]. Further we studied [3,4] the behavior of s as a function of chemical potential, temperature and gap magnitude for the gapped Dirac materials, e.g. silicene, germanene. It was demonstrated in [4] that the disappearance of the characteristic entropy resonance can be considered as a signature of the topological phase transition in germanene. Layered transition-metal dichalcogenides represent another class of materials that can be shaped into monolayers. They are truly two-dimensional (2D) semiconductors with a direct large band gap of the order of 1–2 eV, so that the peaks in the DEP can be seen at much higher temperatures [5]. All these results were summarized in the review article [6].

While in the experimental paper [1] the DEP s of 2D electron gas in perpendicular magnetic field was also investigated, all the above-mentioned theoretical works were limited to the case of zero external magnetic field. In the present work we study the behavior of s in three-dimensional (3D) Dirac semimetals in the presence of quantizing magnetic field.

Dirac semimetals in 3D are three-dimensional analogues of graphene and present a new class of materials with nontrivial topological properties (for a review see, for example, [7] and references therein). Their low-energy fermionic excitations are described by a 3D Dirac Hamiltonian. Historically, bismuth provides the first example of a material whose low-energy quasiparticle excitations at certain point of the Brillouin zone are described by the 3D massive Dirac equation [8–11] while massless Dirac fermions were observed in an alloy $Bi_{1-x}Sb_x$ with the antimony concentration of about $x\approx 0.03$ [12]. Recently, the 3D Dirac fermions were experimentally discovered in

compounds Na_3Bi and Cd_3As_2 [13–15]. We show that the behavior of the DEP as a function of doping in Dirac semimetals in the presence of a magnetic field is significantly different from its behavior in 2D Dirac systems, like graphene.

The paper is organized as follows. We begin by presenting in Sec. 2 the model and discuss the density of states (DOS). The analytical expression for the DEP and numerical results are presented in Sec. 3. In Conclusion, Sec. 4, we summarize the obtained results. The DOS and DEP for a finite scattering rate are derived in Appendix.

2. Models of Dirac semimetals

A Dirac semimetal is a material in which the conduction and valence bands touch only at isolated points within the Brillouin zone (BZ). Near these points the dispersion is linear and the low energy theory is described by a Dirac Hamiltonian. Perhaps the most famous Dirac material is graphene, but Dirac semimetals can also exist in three dimensions. The corresponding low energy Hamiltonian valid in the vicinity of the two Weyl nodes K and K' of opposite chirality reads

$$\mathcal{H}=\begin{pmatrix}\hbar v_F\boldsymbol{\sigma}\mathbf{k} & 0\\ 0 & -\hbar v_F\boldsymbol{\sigma}\mathbf{k}\end{pmatrix}, \tag{2}$$

where v_F is the Fermi velocity, $\boldsymbol{\sigma}=(\sigma_1,\sigma_2,\sigma_3)$ are Pauli matrices, and $\mathbf{k}$ is the waver-vector measured from the K, K' points.

In contrast to graphene, where any perturbation proportional to σ_3 would gap out the band touching, the single Weyl node (K or K') Hamiltonian is robust against such a perturbation since it already uses all three of the Pauli matrices. However, the Hamiltonian (2) of 3D Dirac semimetal is not robust against more general perturbations since there are additional Dirac matrices in the 4×4 representation. The robustness can be imposed by requiring that the Hamiltonian is invariant under time reversal (T) symmetry and inversion symmetry (P). Then there must be four bands linearly dispersing around any band touching point in the BZ. One can easily check that the Dirac semimetal Hamiltonian is invariant under time reversal symmetry

$$T\mathcal{H}^*(-\mathbf{k})T^{-1}=\mathcal{H}(\mathbf{k}),\quad T=\begin{pmatrix}i\sigma_2 & 0\\ 0 & i\sigma_2\end{pmatrix}, \tag{3}$$

and inversion symmetry

$$P\mathcal{H}(-\mathbf{k})P^{-1}=\mathcal{H}(\mathbf{k}),\quad P=\begin{pmatrix}0 & \sigma_0\\ \sigma_0 & 0\end{pmatrix}, \tag{4}$$

where σ_0 is 2×2 unit matrix. In Weyl semimetal at least one of these symmetries is broken. Only the Dirac semimetals are considered in this work.

In an external magnetic field the Hamiltonian (2) acquires the following form in a configurational space:

$$\mathcal{H}=v_F\begin{pmatrix}\boldsymbol{\sigma}\left(-i\hbar\nabla+\dfrac{e}{c}\mathbf{A}\right) & 0\\ 0 & -\boldsymbol{\sigma}\left(-i\hbar\nabla+\dfrac{e}{c}\mathbf{A}\right)\end{pmatrix}. \tag{5}$$

We consider the external magnetic field $\mathbf{B}=\mathbf{B}\hat{z}$ applied along the positive z axis, and use the gauge $A_y=A_z=0$ and $A_x=-By$. The spectrum at K ($\xi=1$) and K' ($\xi=1$) points and is given by the expressions

$$E_{n\xi}=\begin{cases}-\xi\hbar v_F k_z, & n=0,\\ \pm\sqrt{(\hbar v_F k_z)^2+\Delta_n^2}, & n\geq1,\end{cases} \tag{6}$$

where

$$\Delta_n=\sqrt{\frac{2n\hbar v_F^2|eB|}{c}} \tag{7}$$

is the energy scale that characterizes the energies of the Landau levels. The corresponding density of states, $D(\epsilon)$, is defined as

$$D(\epsilon)=\frac{1}{2\pi l^2}\sum_{\xi=\pm}\sum_{n=0}^{\infty}\int_{-\infty}^{\infty}\frac{dk_z}{2\pi}\delta(\epsilon-E_{n\xi}), \tag{8}$$

where $l=\sqrt{\hbar c/|eB|}$ is the magnetic length and $1/2\pi l^2$ is the degeneracy of a Landau level. Integrating Eq. (8) over the wave-vector k_z, one arrives at the expression (cf. Eq. (7) for the DOS for one K point in Ref. 16)

$$D(\epsilon)=\frac{1}{2\pi^2\hbar v_F l^2}\left[1+2\sum_{n=1}^{\infty}\frac{|\epsilon|}{\sqrt{\epsilon^2-\Delta_n^2}}\theta(\epsilon^2-\Delta_n^2)\right]. \tag{9}$$

The first term in square brackets is due to the contribution of zero Landau level. The DOS for the Dirac semimetal in the limit of zero magnetic field can be obtained directly from Eq. (9) by keeping the quantity Δ_n constant, while $B\to0$ and $n\to\infty$. This reproduces the known result

$$D(\epsilon)\to\frac{|\epsilon|}{2\pi^2(\hbar v_F)^3}\int_0^{\epsilon^2}\frac{dx}{\sqrt{\epsilon^2-x}}=\frac{\epsilon^2}{\pi^2(\hbar v_F)^3}. \tag{10}$$

It is instructive to compare Eq. (9) with the DOS (per spin) for the 2D massless Dirac fermions in graphene [17]

$$D_{\rm gr}(\epsilon)=\frac{1}{\pi l^2}\left[\delta(\epsilon)+\sum_{n=1}^{\infty}(\delta(\epsilon-\Delta_n)+\delta(\epsilon+\Delta_n))\right]. \tag{11}$$

The specific of the DOS (11) is that it does not involve integration over momentum and for the clean case contains δ-functions. In Fig. 1 we show both the DOS (9) of the Dirac semimetal (lower panel) and 2D massless Dirac fermions (11) (upper panel) as functions of the energy. The zero field limits are shown too. To represent the DOS in

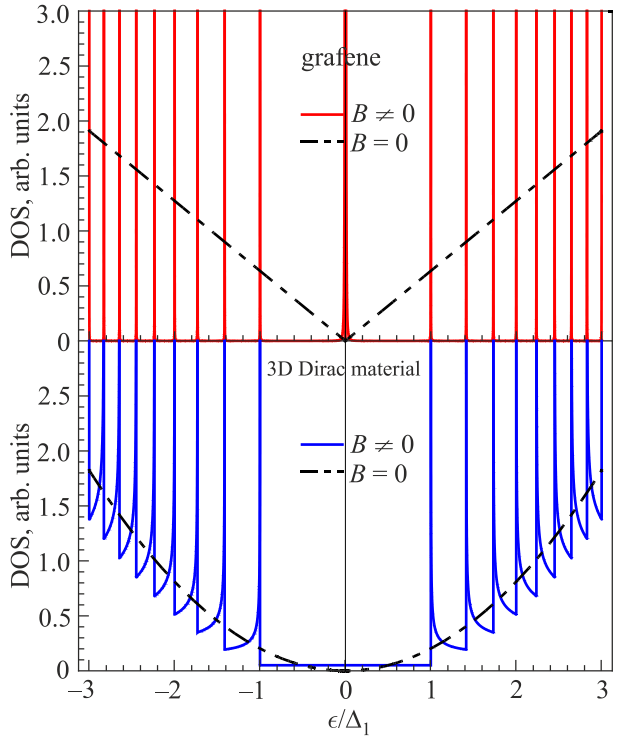

Fig. 1. (Color online) The DOS as a function of energy ϵ in the units of the energy Δ_1 for the Dirac semimetal (lower panel) and graphene (top panel). The 2D Landau levels are broadened by the width $\gamma = 10^{-5}\Delta_1$. The zero field DOS is shown by the dash-dotted lines.

the figure the δ-functions spikes of the 2D DOS were smeared out to the Lorentzians, viz.

$$\delta(\epsilon) \to \frac{\gamma}{\pi[\epsilon^2 + \gamma^2]}, \tag{12}$$

where γ is the scattering rate. Besides the asymmetric shape of the DOS peaks in the 3D case, the specific of the Dirac semimetal is that below the magnetic energy, $|\epsilon| < \Delta_1$, the DOS is identically zero.

3. Differential entropy per particle

As discussed above (see Eq. (1)), the DEP is directly related to the temperature derivative of the chemical potential at a fixed charge density of carriers or carrier imbalance n ($n = n_+ - n_-$, where n_+ and n_- are the densities of electrons and holes, respectively). The DEP can be obtained using the thermodynamic identity

$$s = -\left(\frac{\partial \mu}{\partial T}\right)_n = \left(\frac{\partial n}{\partial T}\right)_\mu \left(\frac{\partial n}{\partial \mu}\right)_T^{-1}. \tag{13}$$

For the DOS being an even function of energy, the charge density of carriers at finite temperature and a magnetic field can be written as [3,17]

$$n(T,\mu,B) = \frac{1}{4}\int_{-\infty}^{\infty} d\epsilon D(\epsilon)\left[\tanh\frac{\epsilon+\mu}{2T} - \tanh\frac{\epsilon-\mu}{2T}\right]. \tag{14}$$

Calculating the derivatives over T and μ and using Eq. (13), we find that the DEP is given by the general relation [2,3,6]:

$$s(\mu,T) = \frac{1}{T}\frac{\int_{-\infty}^{\infty} d\epsilon D(\epsilon)(\epsilon-\mu)\cosh^{-2}\left(\frac{\epsilon-\mu}{2T}\right)}{\int_{-\infty}^{\infty} d\epsilon D(\epsilon)\cosh^{-2}\left(\frac{\epsilon-\mu}{2T}\right)}. \tag{15}$$

Its behavior as a function of chemical potential for 3D Dirac semimetal in a magnetic field at finite temperature is shown in Fig. 2 by blue curve. It follows from Eq. (15) that $s(\mu,T) \to 0$ when $\mu \to 0$. In fact, there is a rather large flat region with almost zero differential entropy, $s(\mu,T) = 0$, near the charge neutral point $\mu = 0$ followed by decreasing oscillations due to contributions from the Landau levels. The behavior near $\mu = 0$ is in sharp contrast to the behavior in graphene in a magnetic field where there is instead a sharp peak observed for the chemical potential in the temperature vicinity of the Dirac point, $|\mu| \sim T$ (red curve in Fig. 2). The prominent peak in graphene is due to the contribution of zero Landau level (compare two DOS, Eq. (9) and Eq. (11)). Oscillations of the DEP as a function of the chemical potential are clearly seen in both systems, and the maxima of oscillations correspond to the chemical potential crossing a Landau level. In the 2D case the DEP oscillates around zero value, because the peaks of the DOS have a symmetric shape, while the asymmetric shape of the 3D Dirac semimetal results in nonzero background value of the DEP.

The dependence of the DEP on the applied magnetic field for 3D Dirac semimetal is shown in Fig. 3. One ob-

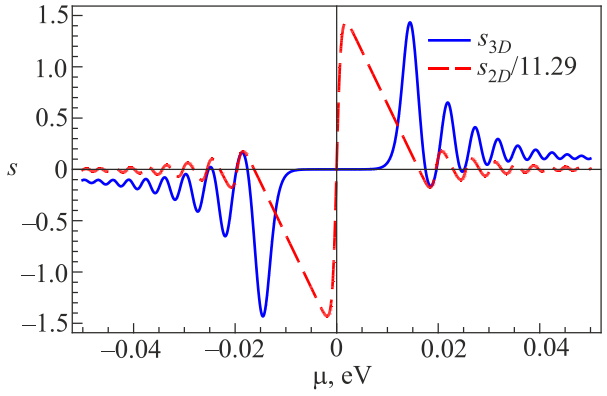

Fig. 2. (Color online) The differential entropy per particle s as a function of the chemical potential μ in eV in the Dirac semimetal (solid blue curve) and graphene (dashed red line). To show both plots on the same graph, the results for graphene are divided by the factor 11.29. The magnetic field $B = 0.2$ T, the temperature $T = 10$ K and the Fermi velocity is $v_F = 10^6$ m/s.

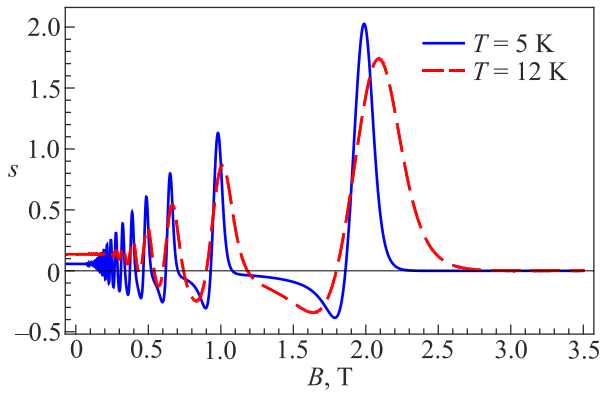

Fig. 3. (Color online) The differential entropy per particle s as a function of the magnetic field B in Tesla in the 3D Dirac semimetal for the two different values of the temperature. The chemical potential $\mu = 0.05$ eV and the Fermi velocity is $v_F = 10^6$ m/s .

serves the oscillatory behavior of the DEP. The amplitude of the oscillations increases as the magnetic field grows. The oscillations disappear when $\Delta_1(B = 2\ \mathrm{T}) \approx 0.05$ eV reaches the value of the Fermi energy. It is also clear that the oscillations are better resolved for the smaller value of the temperature. Similar behavior of the DEP is observed in experiments on 2D electron gas with a parabolic dispersion (see Figs. 1f-h in Ref. 1).

Oscillations in DEP as a function of the carrier density and magnetic field were clearly seen in the experiments with clean two-dimensional electron system in silicon-based structures [1], while similar experiments for 2D and 3D Dirac systems were not performed yet.

The low-temperature expansion for $s(\mu,T)$ can be obtained straightforwardly from Eq. (15) after the change of the variable $\epsilon \to 2T\epsilon + \mu$ and then expanding integrands in series in T. For example, in the first order in temperature we find

$$s(\mu,T) \simeq \frac{\pi^2}{3} T \frac{D'(\mu)}{D(\mu)}. \qquad (16)$$

For finite scattering rate γ one should use the DOS $D(\mu,\gamma)$, Eq. (A.1).

4. Conclusions

In the present paper we studied the DEP for three-dimensional Dirac systems as a function of chemical potential, temperature and magnetic field. This quantity is related through the Maxwell relation to the temperature derivative of the chemical potential, which in turn is measured directly in experiments where modulation of the sample temperature causes recharging of the gated structure [1]. We show that DEP near the charge neutral point has a flat region (plateau). Its size grows with the increase of the magnetic field. Starting from the first Landau level, the DEP oscillates when the chemical potential crosses Landau levels exhibiting Lifshitz-like transitions.

In 2D gapless Dirac systems like graphene, the behavior of the DEP in the vicinity of the charge neutral point $\mu = 0$ is quite different: instead of a plateau there is a big peak when the chemical potential is in the temperature vicinity of the Dirac point. Recently, oscillations in DEP were clearly seen in the experiments with clean two-dimensional electron system in silicon-based structures [1]. We expect that similar experiments for 2D and 3D Dirac systems, not performed yet, might reveal specific features expected in the behavior of the DEP in the applied magnetic field.

Acknowledgments

The work of S.G.Sh. and V.P.G. was partly supported by the Ukrainian-Israeli Scientific Research Program of the Ministry of Education and Science of Ukraine (MESU) and the Ministry of Science and Technology of the State of Israel (MOST), and by the National Academy of Sciences of Ukraine (projects Nos. 0117U000236 and 0116U003191).

Appendix
DOS and charge carrier density for 3D Dirac systems in a magnetic field at finite scattering rate

For a constant scattering rate γ, and using the Lorentzian broadening of each Landau level, Eq. (12), the DOS (8) can be written as

$$D(\epsilon,\gamma) = \frac{1}{2\pi^2 \hbar v_F l^2} \left\{ 1 + \frac{2\gamma}{\pi} \sum_{n=1}^{\infty} \int_{\Delta_n}^{\infty} \frac{dx x}{\sqrt{x^2 - \Delta_n^2}} \times \right.$$
$$\left. \times \left[\frac{1}{(x+\epsilon)^2 + \gamma^2} + \frac{1}{(x-\epsilon)^2 + \gamma^2} \right] \right\}. \qquad (A.1)$$

The integral can be evaluated through elementary functions, but is better to keep it in the current compact form. Clearly, for $\gamma = 0$ the DOS reduces to Eq. (9). This expression for DOS is used for numerical calculation of the entropy per particle (15) at finite scattering rate. More convenient expression for the entropy per particle can be obtained evaluating integrals over energy. We calculate first the charge carrier density (14) with the DOS $D(\epsilon,\gamma)$ from (A.1) using the integral

$$\int_{-\infty}^{\infty} \frac{dx \tanh x}{(x+a)^2 + b^2} = \frac{2}{|b|} \mathrm{Im}\, \Psi\left(\frac{1}{2} + \frac{|b| - ia}{\pi} \right), \qquad (A.2)$$

where $\Psi(z)$ is the digamma function. The last one can be derived using

$$\tanh x = 2 \sum_{n=0}^{\infty} \frac{x}{\pi^2 (n+1/2)^2 + x^2}, \qquad (A.3)$$

integrating over x, and evaluating then the sum. We obtain

$$n(T,\mu,B,\gamma)=\frac{1}{2\pi^2\hbar v_F l^2}\left\{\mu+\frac{2}{\pi}\sum_{n=1}^{\infty}\int_{\Delta_n}^{\infty}\frac{dxx}{\sqrt{x^2-\Delta_n^2}}\times\right.$$

$$\left.\times\,\mathrm{Im}\left[\Psi\left(\frac{1}{2}+\frac{\gamma+i(\mu+x)}{2\pi T}\right)-\Psi\left(\frac{1}{2}+\frac{\gamma+i(-\mu+x)}{2\pi T}\right)\right]\right\}. \tag{A.4}$$

For the derivatives we find

$$\frac{\partial n(T,\mu,B,\gamma)}{\partial T}=\frac{1}{\pi^4\hbar v_F l^2 T}\sum_{n=1}^{\infty}\int_{\Delta_n}^{\infty}\frac{dxx}{\sqrt{x^2-\Delta_n^2}}\times$$

$$\times\,\mathrm{Im}\left[\frac{\gamma+i(-\mu+x)}{2T}\Psi'\left(\frac{1}{2}+\frac{\gamma+i(-\mu+x)}{2\pi T}\right)-\right.$$

$$\left.-\frac{\gamma+i(\mu+x)}{2T}\Psi'\left(\frac{1}{2}+\frac{\gamma+i(\mu+x)}{2\pi T}\right)\right], \tag{A.5}$$

$$\frac{\partial n(T,\mu,B,\gamma)}{\partial\mu}=\frac{1}{2\pi^2\hbar v_F l^2}\times$$

$$\times\left\{1+\frac{1}{\pi^2 T}\sum_{n=1}^{\infty}\int_{\Delta_n}^{\infty}\frac{dxx}{\sqrt{x^2-\Delta_n^2}}\mathrm{Re}\left[\Psi'\left(\frac{1}{2}+\frac{\gamma+i(-\mu+x)}{2\pi T}\right)+\right.\right.$$

$$\left.\left.+\Psi'\left(\frac{1}{2}+\frac{\gamma+i(\mu+x)}{2\pi T}\right)\right]\right\}. \tag{A.6}$$

The differential entropy per particle is calculated then by means of Eq. (13). The limit of zero scattering rate, $\gamma=0$, is obtained by using the formula

$$\mathrm{Re}\,\Psi'\left(\frac{1}{2}+ix\right)=\frac{\pi^2}{2}\frac{1}{\cosh^2\pi x}. \tag{A.7}$$

In the first order expansion in T we obtain from Eqs. (A.5) and (A.6)

$$\frac{\partial n(T,\mu,B,\gamma)}{\partial T}\simeq\frac{2T\gamma}{3\pi^2\hbar v_F l^2}\sum_{n=1}^{\infty}\int_{\Delta_n}^{\infty}\frac{dxx}{\sqrt{x^2-\Delta_n^2}}\times$$

$$\times\left[\frac{x-\mu}{[(x-\mu)^2+\gamma^2]^2}-\frac{x+\mu}{[(x+\mu)^2+\gamma^2]^2}\right]=$$

$$=\frac{\pi^2 T}{3}\frac{dD(\mu,\gamma)}{d\mu},\quad T\to 0, \tag{A.8}$$

$$\frac{\partial n(T,\mu,B,\gamma)}{\partial\mu}=D(\mu,\gamma),\quad T\to 0. \tag{A.9}$$

The differential entropy per particle is given by Eq. (16) with the DOS dependent on γ, Eq. (A.1).

1. A.Yu. Kuntsevich, V.M. Pudalov, I.V. Tupikov, and I.S. Burmistrov, *Nat. Commun.* **6**, 7298 (2015).
2. A.A. Varlamov, A.V. Kavokin, and Y.M. Galperin, *Phys. Rev. B* **93**, 155404 (2016).
3. V.Yu. Tsaran, A.V. Kavokin, S.G. Sharapov, A.A. Varlamov, and V.P. Gusynin, *Sci. Rep.* **7**, 10271 (2017).
4. D. Grassano, O. Pulci, V.O. Shubnyi, S.G. Sharapov, V.P. Gusynin, A.V. Kavokin, and A.A. Varlamov, *Phys. Rev. B* **97**, 205442 (2018).
5. V.O. Shubnyi, V.P. Gusynin, S.G. Sharapov, and A.A. Varlamov, *Fiz. Nizk. Temp.* **44**, 721 (2018) [*Low Temp. Phys.* **44**, 561 (2018)].
6. Y.M. Galperin, D. Grassano, V.P. Gusynin, A.V. Kavokin, O. Pulci, S.G. Sharapov, V.O. Shubnyi, and A.A. Varlamov, *J. Exp. Theor. Phys.* **127**, 958 (2018).
7. T.O. Wehling, A.M. Black-Schaffer, and A.V. Balatsky, *Adv. Phys.* **63**, 1 (2014).
8. M.H. Cohen and E.I. Blount, *Philos. Mag.* **5**, 115 (1960).
9. P.A. Wolff, *J. Phys. Chem. Solids* **25**, 1057 (1964).
10. L.A. Fal'kovskii, *Sov. Phys. Usp.* **11**, 1 (1968) [*Usp. Fiz. Nauk* **94**, 3 (1968)].
11. V.S. Edel'man, *Sov. Phys. Usp.* **20**, 819 (1977) [*Usp. Fiz. Nauk* **123**, 257 (1977)].
12. B. Lenoir, M. Cassart, J.-P. Michenaud, H. Scherrer, and S. Scherrer, *J. Phys. Chem. Solids* **57**, 89 (1996).
13. Z.K. Liu, B. Zhou, Z.J. Wang, H.M. Weng, D. Prabhakaran, S.-K. Mo, Y. Zhang, Z.X. Shen, Z. Fang, X. Dai, Z. Hussain, and Y.L. Chen, *Science* **343**, 864 (2014).
14. M. Neupane, Su-Yang Xu, R. Sankar, N. Alidoust, G. Bian, C. Liu, I. Belopolski, T.-R. Chang, H.-T. Jeng, H. Lin, A. Bansi, F. Chou, and M.Z. Hasan, *Nature Commun.* **5**, 3786 (2014).
15. S. Borisenko, Q. Gibson, D. Evtushinsky, V. Zabolotnyy, B. Büchner, and R.J. Cava, *Phys. Rev. Lett.* **113**, 027603 (2014).
16. P.E.C. Ashby and J.P. Carbotte, *Eur. Phys. J. B* **87**, 92 (2014).
17. S.G. Sharapov, V.P. Gusynin, and H. Beck, *Phys. Rev. B* **69**, 075104 (2004).

Диференціальна ентропія на частинку в дираківському напівметалі в зовнішньому магнітному полі

І.В. Сухенко, С.Г. Шарапов, В.П. Гусинін

Для тривимірних дираківських систем отримано загальний вираз, що описує диференційну ентропію на частинку (ДЕЧ) в залежності від хімічного потенціалу, температури та магнітного поля. Показано, що в присутності магнітного поля залежність ДЕЧ від хімпотенціалу поблизу зарядово-нейтральної точки істотно відрізняється від відповідної залежності у графені. Зокрема, поблизу нейтральної точки заряду спостерігається плато з майже нульовою ДЕЧ, яке роз-

ширюється зі збільшенням магнітного поля, а потім виникають осциляції, що згасають, пов'язані з внеском рівнів Ландау. Навпаки, у графені спостерігається гострий пік хімпотенціалу поблизу температури точки Дірака.

Ключові слова: 3D діраківські системи, диференціальна ентропія, хімічний потенціал, магнітне поле.

Дифференциальная энтропия на частицу в дираковском полуметалле во внешнем магнитном поле

И.В. Сухенко, С.Г. Шарапов, В.П. Гусынин

Для трехмерных дираковских систем получено общее выражение, описывающее дифференциальную энтропию на частицу (ДЭЧ) в зависимости от химического потенциала, температуры и магнитного поля. Показано, что в присутствии магнитного поля зависимость ДЭЧ от химпотенциала вблизи зарядово-нейтральной точки существенно отличается от соответствующей зависимости в графене. В частности, вблизи нейтральной точки заряда наблюдается плато с почти нулевой ДЭЧ, которое расширяется с увеличением магнитного поля, а затем возникают затухающие осцилляции, связанные с вкладом уровней Ландау. Напротив, в графене наблюдается острый пик химпотенциала вблизи температуры точки Дирака.

Ключевые слова: 3D дираковские системы, дифференциальная энтропия, химический потенциал, магнитное поле.